LEGIBILITY NOTICE

A major purpose of the Technical Information Center is to provide the broadest dissemination possible of information contained in DOE's Research and Development Reports to business, industry, the academic community, and federal, state and local governments.

Although a small portion of this report is not reproducible, it is being made available to expedite the availability of information on the research discussed herein.

LA-UR-90-2843

Los Alamos National Laboratory is operated by the University of California for the United States Department of Energy under contract W-7405-ENG-36

LA-UR--90-2843

DE90 016486

TITLE ANALYSIS OF CONTAMINANT MOVEMENT AT DIFFERENT EXPERIMENTAL SCALES

AUTHOR(S) E. P. Springer, T. B. Stauffer, W. G. MacIntyre, B. D. Newman, and C. A. Antworth

SUBMITTED TO HAZTECH International 1990 Conf.,
Pittsburgh, PA
October 2, 1990

DISCLAIMER

Los Alamos National Laboratory
Los Alamos, New Mexico 87545

ANALYSIS OF CONTAMINANT MOVEMENT AT DIFFERENT EXPERIMENTAL SCALES

E. P. Springer[1], T. B. Stauffer[2], W. G. MacIntyre[3], B. D. Newman[1], and C. A. Antworth[2]

ABSTRACT

Two experimental approaches were used to examine transport in saturated porous media. One design, the box experiment, allowed two-dimensional sampling of the solute plume. The more traditional column design was one-dimensional with sample collection only at the effluent end. A total of three box and two column experiments were conducted. The method of moments was used to analyze plume behavior in both experiments. Comparison between the experiments were made using the moments. For similar porous materials the same retardation was observed despite an order of magnitude difference in velocities. Data from the one-dimensional column experiments were used to estimate dispersivities that were used to predict the behavior in the multidimensional box experiment. Results indicated that velocity information from the box experiment was needed in order to atain an adequate prediction of its response.

INTRODUCTION

Effective remediation of contaminated aquifers requires knowledge of physical and chemical properties governing transport of the contaminant of interest. Experiments are conducted at the laboratory or bench scale to define processes and parameters controlling these processes in order to design a mitigation strategy. Research has shown that heterogeneities at the field scale cause much larger spreading than predicted from bench scale experiments. The recognition of scale dependency in parameters governing transport has led to field-scale experiments to describe behavior of contaminants in heterogeneous and multidimensional systems (see Mackay et al. 1986). A continuing problem is that field-scale studies are expensive and difficult to conduct with chemicals that are hazardous.

[1]Environmental Science Group, MS J495, Los Alamos National Laboratory, Los Alamos, NM 87545.

[2]HQ Air Force Engineering and Services Center, HQ AFESC/RDVW, Tyndall AFB, FL 32403 6001.

[3]School of Marine Science, College of William and Mary, Gloucester Point, VA 23067.

One approach to rectifying differences observed between field and laboratory behavior of contaminants is by conducting experiments at various scales to determine applicability of various models and their parameter values as the experimental conditions change. This approach is being pursued by the Air Force Engineering and Services Center (AFESC) and Los Alamos National Laboratory. This paper will summarize work that has been completed to date and assess the implications of these data.

METHODS

Box Experiments

One of the key features in dispersion of a contaminant plume is the presence of multidimensional flow paths. Many column experiments are conducted so that one-dimensional flow is forced due to the diameter of the column. The experimental design used here is basically a glass box filled with aquifer material. By injecting a tracer at a point, the plume can develop and thus three-dimensional behavior can be observed.

The dimensions of the box are 152.4 cm long X 30.5 cm high X 30.5 cm wide. A 200 mesh screen was installed 5.1 cm from each end of the box to form reservoirs for flow control through the box. The remaining interval of 142.2 cm was filled to a height of 26.7 cm with aquifer material. A schematic of the box layout is shown in Figure 1.

Rows of sampling wells made of heavy walled glass tubing were installed at distances of 10.2, 15.2, 20.3, 30.2, 40.3, 50.2, 60.3, 70.2, 80.3, 90.5, 100.6, 110.8, and 130.2 cm from the up-gradient end of the box (Figure 1). Generally, five wells were located across the box at each distance to provide a lateral measure of tracer spread. For the sampling locations between 0-30.2 cm, the lateral wells were located at 11.4, 15.6, and 19.7 cm from the right-hand wall looking in the down gradient direction (Figure 1). For the remaining distances, there were five lateral wells at each sampling distance and these were located at 5.1, 10.2, 15.2, 20.3, and 25.4 cm from the same wall.

Prior to injecting tracer, a steady state flow field was established by maintaining constant water elevation in each end reservoir thus creating a constant gradient. The tracers were injected into the well located at x=15.2 cm and y -15.2cm. Samples were taken in all down-gradient wells at various time intervals depending on the flow rate used in the experiment.

Tracers used in these experiments were tritiated water and C^{14} labelled naphthalene. Each sample was counted to determine activity. Tritiated water was used as the nonreactive tracer to determine physical transport parameters. The naphthalene was retarded relative to the flow of the tritiated water.

The solid materials placed into the three box experiments were a sand in experiments 1 and 2, and experiment 3 used aquifer material obtained from the saturated zone at Columbus AFB in Mississippi. The aquifer material was sieved and the less than 2 mm fraction was used because it was assumed to be the most reactive component of the aquifer material.

Column Experiments

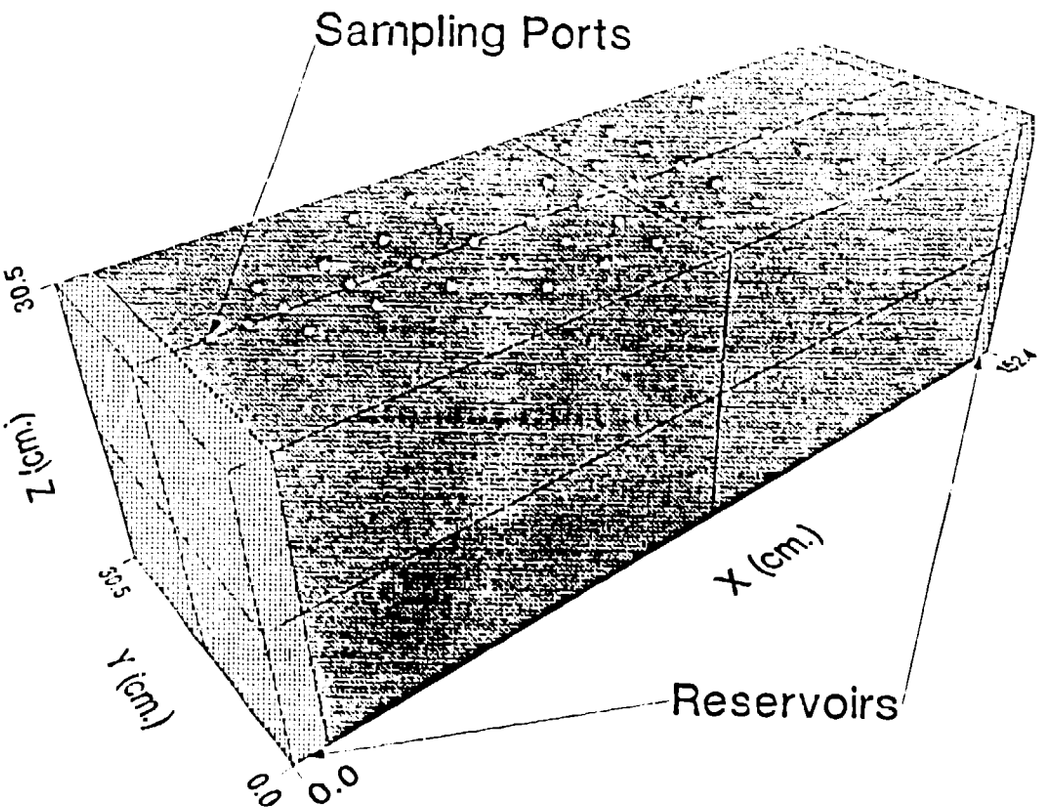

Figure 1. Physical setup for box experiments.

Column experiments have traditionally been used to determine transport parameters and chemical interactions in dynamic systems. Columns have represented one-dimensional flow systems because the relatively small diameter does not permit lateral flow variations.

The column used in this phase of the project was 100 cm long and 15 cm in diameter Pyrex glass cylinder. A fritted glass plate was used at the effluent end. The less than 2 mm aquifer material was used to pack the column to a bulk density of 1.523 g/cm^3. The column was packed as carefully as possible in 2-cm lifts to allow compaction of the material and avoid separation upon filling the column with solution.

Influent solution was prepared to simulate the groundwater conditions at Columbus AFB with a pH of 5.5 and an ionic strength of 0.0007. After steady state conditions were established, a pulse of lithium bromide tracer was injected. Bromide was the nonreactive tracer and lithium was the reactive tracer. In column experiment 1, the input pulse was 3-hours duration and for column experiment 2, the pulse was 6-hours duration. Grab samples for lithium were collected at the outlet at least three times daily and lithium was analyzed using an ion chromatograph. Bromide measurements were taken every 30 sec. with a bromide specific electrode controlled by a microcomputer in a flow through cell attached to the outlet of the column.

Analysis

Analyses of these experiments used the method of moments. The method of moments is preferred because no assumptions are made about an underlying model. The following analyses used both spatial and temporal moments. Both spatial and temporal moments were used with the box data because multiple spatial samples were collected at a given time. Only temporal moments were applied to the column data since samples were only collected at the outlet of the column.

Moments are estimated from the data by integrating in space or time. The Nth temporal moment is defined as:

$$M_T^n = \int_0^{T_f} \tau^N \, C(x,\tau) \, q(\tau) d\tau$$

where M_T^n is the Nth temporal moment, $C(x,\tau)$ is the solute concentration at the time τ; τ is a dummy variable of integration; $q(\tau)$ is the flow rate; and T_f is the total duration of the experiment. The zero moment is the total mass of material, and it can be used to normalize the other moments. Low order moments (first, second, and third) are usually estimated because of errors incurred when numerically integrating terms with larger exponents. By normalizing the moments, the first temporal moment gives the average time; the second moment gives the spread; and third moment gives the skewness of the breakthrough curve. Turner (1972) described the use of the temporal moments to analyze breakthrough curves for various situations.

The spatial moments as the term implies, is the spatial integration of the concentrations at a given time. Freyberg (1986) described the analysis of

the field experiment conducted at the Borden site using spatial moments. The spatial moments are defined as:

$$M_{jkl} = \int_{-\infty}^{\infty} \int_{-\infty}^{\infty} \int_{-\infty}^{\infty} x^j\, y^k\, z^1 \phi\, C(x, y, z, t)\, d_x\, d_y\, d_z$$

where M_{jkl} is the spatial moment of noted order, x^j, y^k, and z^1 are the coordinates for j, k, and the 1th moments; ϕ is the porosity; and C(x, y, z, t) is the concentration. The zero moment again defines the total mass in the system.

The numerical integration of Equation 2 required a grid of regularly spaced values for computation. After creating the regular grid using a two-dimensional interpolation, the integration was performed using the formula 25.4.62 from Abramowitz and Stegun (1972). As with the temporal moments, the spatial moments can be normalized by dividing the value by the mass or zero moment (M_{000}). The first spatial moment gives the location of the center of mass and the second spatial moment can be used to describe the spread of the plume.

In deriving the spatial moments, one of the key assumptions was that the counts were assumed to be depth averaged at each well. This is because the sampling in the x-y plane considered only a single depth. Z-coordinate variations were not measured. Therefore, spatial moments in only the x-y coordinate plane are presented in the following analysis.

RESULTS

Box Experiments

For each experiment, samples were taken at different times depending on the flow rate. In box 1, experiment number 1 in the box series, a total of 16 sampling times were used over a 75-hour experimental duration. The box 2 experiment lasted 402 hours with a total of 10 sampling times. There were 5 sampling times in box 3 over a 173-hour duration. For each sampling time all wells were sampled giving a total of 48 samples per sampling time.

These data were used to illustrate plume behavior as shown in Figures 2 and 3. Figure 2 is the tritiated water data for box 2 from sampling times at 30 hours (Figure 2a), at 112 hours (Figure 2b), at 235 hours (Figure 2c), and 354 hours (Figure 2d). The plots reveal a split in the plume at 112 hours (Figure 2b), but this may be an artifact of the interpolation routine used to create the regular grid. Overall the tritiated water appeared to be well behaved. Figure 3 shows the C^{14} counts representing the naphthalene for the same time steps (Figures 3a-3d) as the tritiated water for box 2. The effects of the retardation on the naphthalene movement can be observed, particularly in the later time steps, by the distribution of concentrations above background throughout the domain and by the relative velocity of the peak counts relative to the tritiated water velocity (compare figures 2d and 3d).

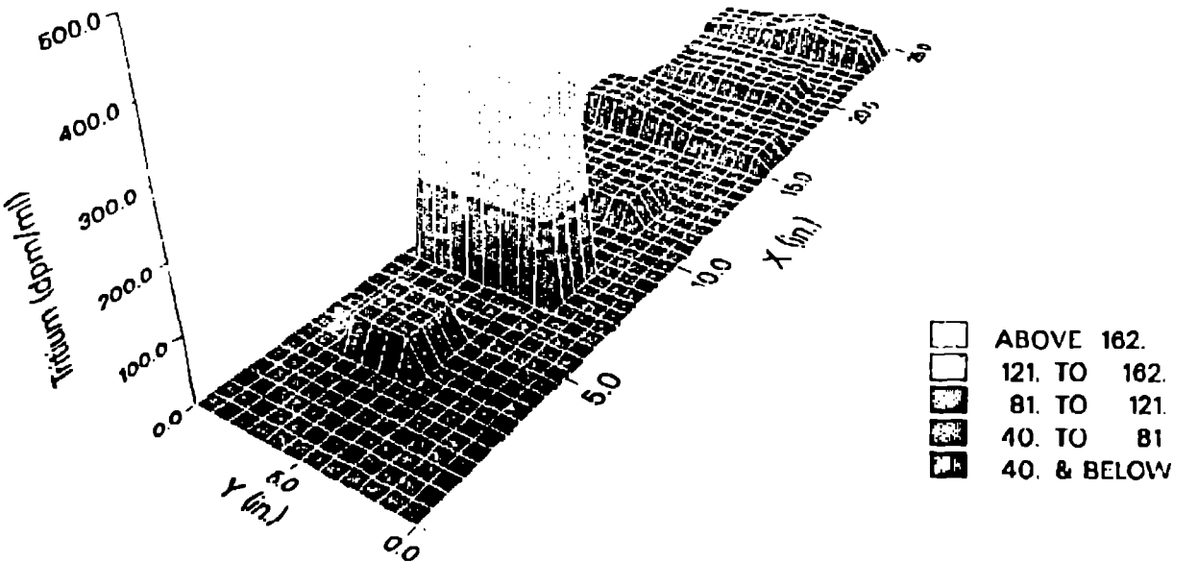

Figure 2a. Perspective plot of tritium activity from box 2 at 30 hours.

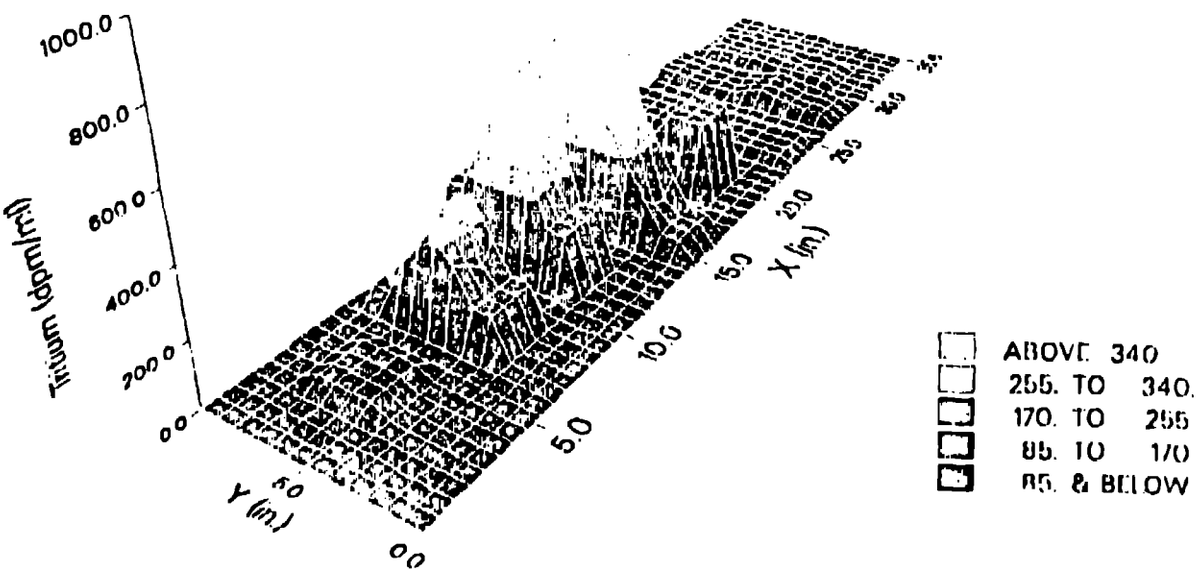

Figure 2b. Perspective plot of tritium activity from box 2 at 112 hours.

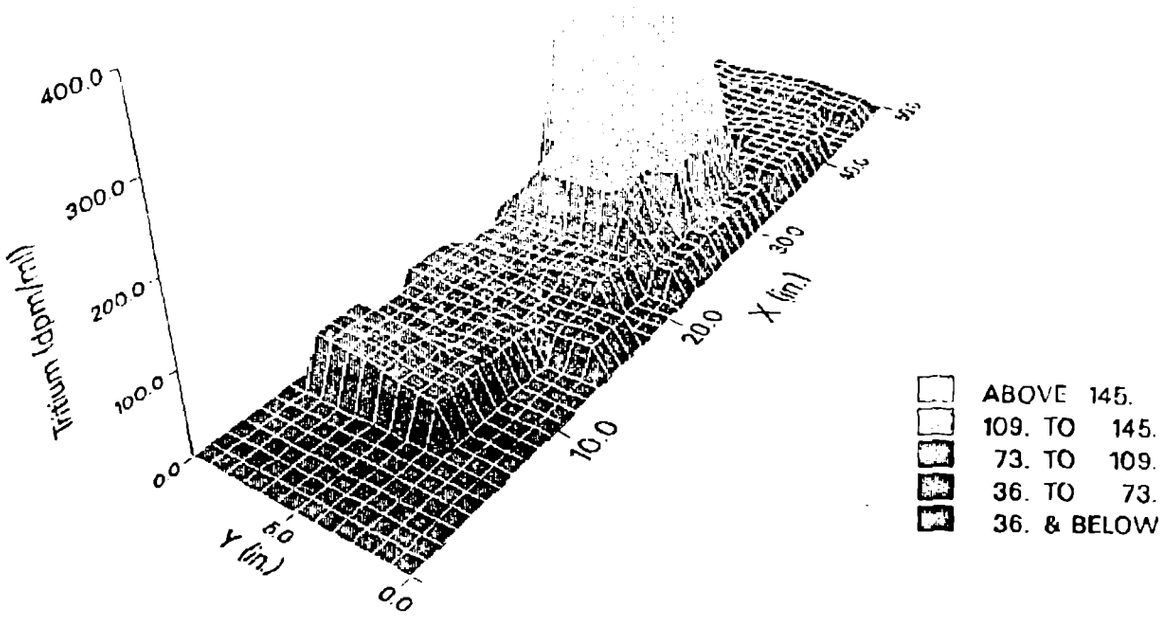

Figure 2c. Perspective plot of tritium activity from box 2 at 235 hours.

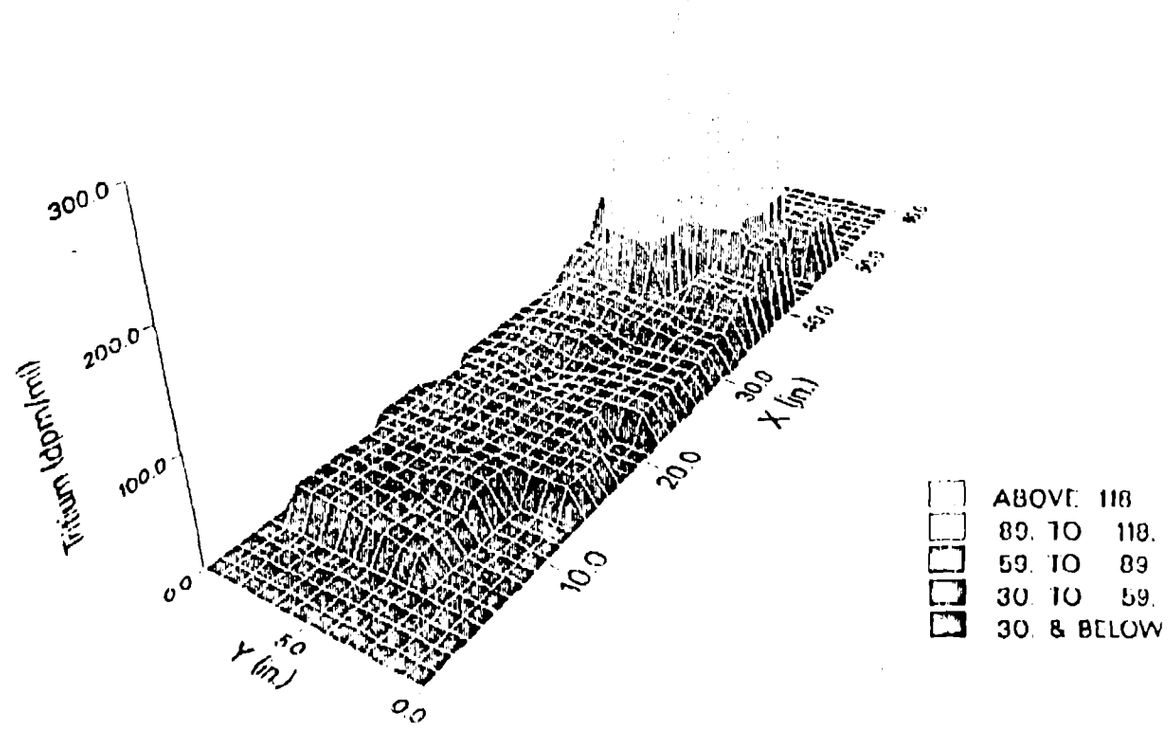

Figure 2d. Perspective plot of tritium activity from box 2 at 354 hours.

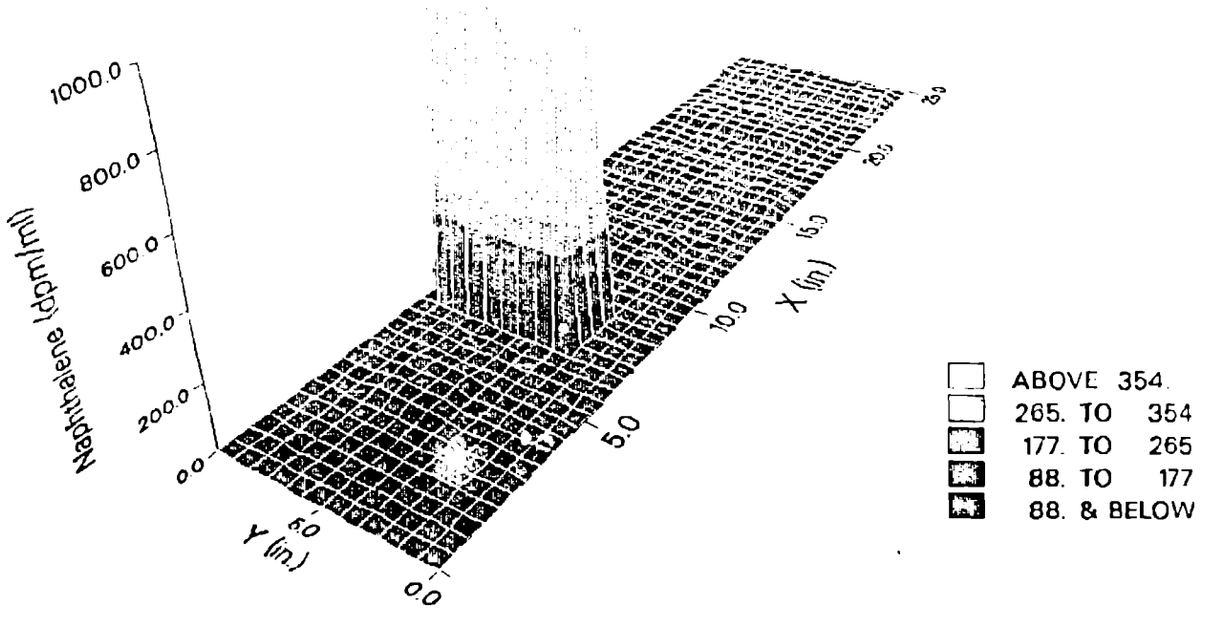

Figure 3a. Perspective plot of naphthalene (C^{14}) activity from box 2 at 30 hours.

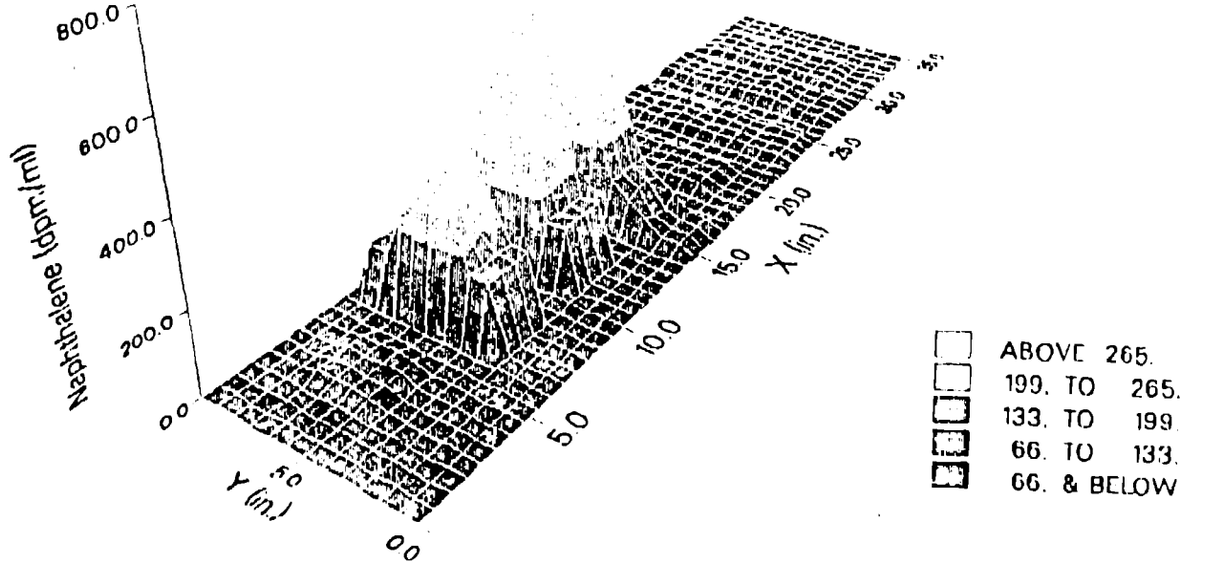

Figure 3b. Perspective plot of naphthalene (C^{14}) activity from box 2 at 112 hours.

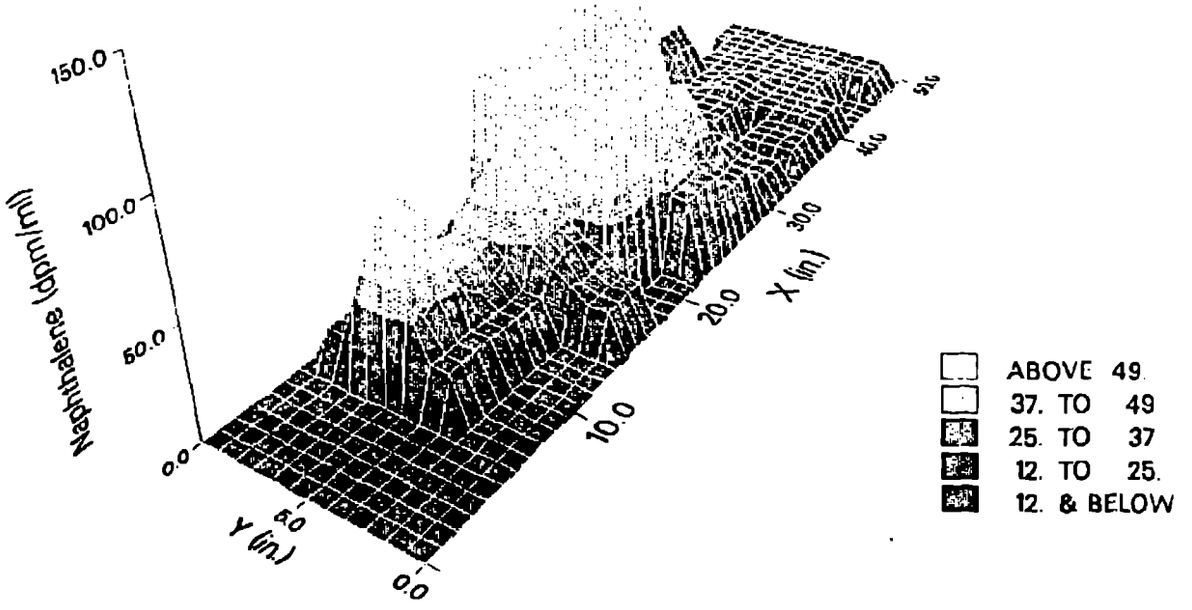

Figure 3c. Perspective plot of naphthalene (C^{14}) activity from box 2 at 235 hours.

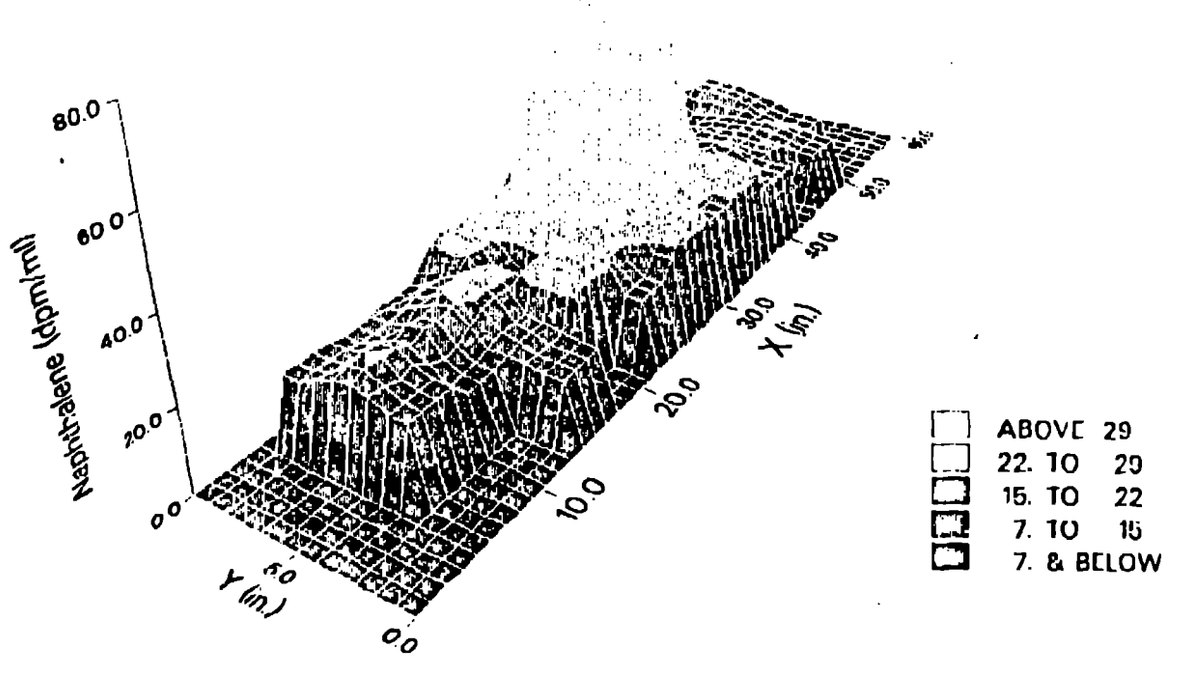

Figure 3d. Perspective plot of naphthalene (C^{14}) activity from box 2 at 354 hours.

Spatial Moments

The normalized first spatial moments are presented in Tables 1, 2, and 3, for box experiments 1, 2, and 3 respectively. One of the first things to note for all three experiments is the y coordinate for the center of mass is very close to the 15-cm center line of the box for both the tritiated water and naphthalene in all three experiments.

The essentially constant value of the y-coordinate and depth averaging in the z coordinate means that displacement can be measured only in the x direction. The velocity of the plume can be determined by fitting a continuous function to the first spatial moment of the following form (Freyberg 1986):

$$X_c(t) = at$$

where X_c is the normalized first movement at time (t); a is a coefficient; and t is time and differentiating with respect to time,. Using linear least-squares, values of a were estimated for both tritium and naphthalene for all three box experiments. These estimates are given in Table 4. Note the higher velocity in box 1 versus the box 2 and 3 experiments. An estimate of retardation, the R value in Table 4, of the naphthalene is given by dividing the tritium velocity by the naphtalene velocity. The estimated R factors for box experiments 1 and 2 are similar as expected given that both were conducted using the same silica sand material. The box 3 R factor is lower reflecting less retardation by the Mississippi aquifer material.

In box 1 a decrease in the value of X_c with time can be seen beginning with the 51-hour sample (Table 1). This decrease was attributed to the absorbing downstream boundary and to the loss of mass.

Normalized second moments for all three box experiments are given in Tables 5, 6, and 7. Again as with the first moments the second moment values remain essentially constant. Also, the magnitude of the second moment in the x direction decreases beginning with the 51-hour sampling time as was observed for the first moment (Table 1).

The variance of the plume which is a measure of the spread in a given direction can be estimated from the first and second normalized moments by:

$$\sigma^2_{ii} = M2_{ii} - (M1_{ii})^2$$

where: σ_{ii} is the estimated variance in coordinate direction i (x, y, or z); $M2_{ii}$ is the normalized second moment; and $M1_{ii}$ is the normalized first moment. Using the values in Tables 1-3 and Tables 5-7, the variance in the x direction was calculated for both tritium and naphthalene for all three box experiments, and these are given in Table 8. The general trend is for increased longitudinal spreading as time progresses. The tritium values in box 1 appear

Table 1. Normalized first spatial moments for box 1.

----- Tritium -----			--- Napthalene ---	
Time (hr)	Xc (cm)	Yc (cm)	Xc (cm)	Yc (cm)
3.0	8.40	13.96	6.47	13.76
7.0	14.35	15.63	9.45	15.77
11.0	20.50	16.10	18.16	16.42
15.0	32.31	14.77	26.19	15.20
19.0	44.30	15.53	36.63	14.55
23.0	52.04	15.72	43.18	15.49
27.0	64.24	15.34	49.10	15.28
31.0	75.77	15.51	57.23	15.66
35.0	85.14	15.38	68.10	15.56
39.0	92.08	16.09	76.56	15.47
45.0	106.43	16.58	85.01	15.58
51.0	85.85	16.00	93.78	16.43
57.0	59.51	16.85	86.56	15.81
63.0	60.48	14.18	77.95	16.18
69.0	58.34	16.70	72.24	16.01
75.0	58.09	15.34	66.27	16.08

Table 2. Normalized first spatial moments for box 2.

----- Tritium -----			----- Napthalene -----	
Time (hr)	Xc (cm)	Yc (cm)	Xc (cm)	Yc (cm)
30.0	9.00	15.99	7.99	16.09
70.0	12.69	16.06	10.66	16.14
112.0	23.80	16.10	18.18	16.16
152.0	32.89	16.09	24.60	16.18
194.0	44.98	16.09	35.38	16.30
235.0	52.81	16.31	46.66	16.15
272.0	63.20	15.94	53.37	16.22
312.0	68.96	15.94	55.70	15.94
354.0	74.47	15.92	59.23	15.95
402.0	82.93	16.30	66.55	15.25

Table 3. Normalized first spatial moments for box 3.

----- Tritium -----			----- Napthalene -----	
Time (hr)	Xc (cm)	Yc (cm)	Xc (cm)	Yc (cm)
78.0	35.17	13.90	28.37	13.01
101.0	46.18	15.23	37.90	14.19
125.0	50.09	15.39	47.14	14.07
149.0	51.41	15.56	55.58	14.12
173.0	75.72	15.25	62.66	14.32

Table 4. Velocities from spatial moments and retardation factors for box experiments.

Experiment	Tritium (cm/hr)	Napthalene (cm/hr)	Retardation
Box 1	2.36	1.88	1.26
Box 2	0.23	0.18	1.29
Box 3	0.41	0.38	1.07

Table 5. Normalized second spatial moments for box 1.

Time (hr)	Tritium M200 (cm**2)	Tritium M020 (cm**2)	Tritium M110 (cm**2)	Napthalene M200 (cm**2)	Napthalene M020 (cm**2)	Napthalene M110 (cm**2)
3.0	162.06	231.42	125.74	76.71	221.87	92.39
7.0	349.93	286.26	221.61	136.52	279.55	154.52
11.0	535.42	303.81	320.32	407.61	301.74	291.16
15.0	1222.58	265.03	459.55	801.29	271.03	381.29
19.0	2078.71	278.45	670.97	1506.45	251.81	516.32
23.0	2832.25	283.81	789.03	2048.38	275.48	652.26
27.0	4364.51	272.53	950.32	2676.77	270.39	732.22
31.0	5915.47	277.29	1129.03	3719.35	283.10	871.61
35.0	7451.60	274.45	1256.77	5097.41	277.74	1022.58
39.0	8974.18	301.55	1402.58	6333.54	275.87	1138.06
45.0	11696.75	319.03	1714.19	7896.76	281.61	1290.00
51.0	8716.11	309.93	1349.03	9690.30	314.39	1504.51
57.0	4594.83	362.84	980.00	8709.66	296.71	1356.77
63.0	4688.38	276.58	804.51	7419.34	304.97	1238.06
69.0	4393.54	345.16	936.77	6567.73	300.19	1137.42
75.0	4512.25	309.35	911.61	5712.25	302.64	1058.06

Table 6. Normalized second spatial moments for box 2.

Time (hr)	Tritium M200 (cm**2)	Tritium M020 (cm**2)	Tritium M110 (cm**2)	Napthalene M200 (cm**2)	Napthalene M020 (cm**2)	Napthalene M110 (cm**2)
30.0	191.10	295.93	143.03	144.32	297.61	131.35
70.0	295.81	299.29	203.94	234.13	299.23	173.29
112.0	774.84	311.16	376.71	535.16	304.90	290.45
152.0	1332.26	319.42	516.19	886.45	312.97	391.61
194.0	2416.77	322.97	702.58	1841.29	325.16	555.68
235.0	3338.70	329.48	835.48	2894.19	326.58	738.71
272.0	4618.70	318.64	983.87	3685.80	329.03	846.45
312.0	5418.05	319.74	1066.45	3938.70	322.45	867.74
354.0	6258.05	319.74	1150.97	4355.99	324.00	925.80
402.0	7812.89	333.03	1314.84	5327.09	299.35	963.22

Table 7. Normalized second spatial moments for box 3.

	Tritium			Napthalene		
Time (hr)	M200 (cm**2)	M020 (cm**2)	M110 (cm**2)	M200 (cm**2)	M020 (cm**2)	M110 (cm**2)
78.0	1761.93	237.40	496.13	1120.64	211.23	362.06
101.0	2787.09	282.06	683.87	1869.67	245.93	526.19
125.0	3642.57	293.81	716.77	2887.09	246.39	638.77
149.0	3834.83	305.61	756.13	3957.41	248.39	749.03
173.0	6790.66	291.28	1104.51	4967.70	255.81	856.77

Table 8. Variance of plume at for tritium and naphthalene for box experiments

Time (hr)	Tritium (CM2)	Naphthalene (CM2)
	--Box 1--	
3	91.46	34.89
7	144.13	47.14
11	115.05	77.97
15	178.72	115.51
19	116.43	164.93
23	123.60	183.87
27	238.17	266.14
31	174.65	444.51
35	202.64	460.15
39	496.37	472.78
45	370.25	669.41
51	1345.55	896.21
57	1053.13	1216.47
63	1030.86	1342.73
69	989.54	1349.46
75	1137.82	1320.72
	--Box 2--	
30	110.11	80.51
70	134.84	120.59
112	208.29	204.60
152	250.31	281.04
194	393.03	589.39
235	550.17	717.05
272	625.07	837.93
312	662.43	835.97
354	711.85	851.47
402	935.33	898.45
	--Box 3--	
78	75.42	315.68
101	654.76	433.51
125	1133.69	664.69
149	1191.88	868.81
173	976.54	1041.23

to fluctuate more than the other two experiments which may be the result of a higher flow rate. After the 45-hour sampling time, the box 1 results are suspect due to the already noted effluent boundary condition.

Temporal Moments

The temporal moments used only sampling wells along the centerline (y=15.24 cm) of each box experiment. This approach is supported by the analysis of the normalized first spatial moments in Tables 1-3 that indicate the coordinate for the center of mass in the y direction is very near the 15 cm centerline of the box.

An example of the breakthrough curve used to determine the temporal moments is given in Figure 4. The integration was done using a two-point Gauss-Legendre integration algorithm (Carnahan et al. 1969).

The first and second normalized temporal moments are given in Tables 9, 10 , and 11 for box experiments 1, 2, and 3, respectively. The most obvious difference among the experiments is the higher values for the first and second moments in box 2 versus box 1 and 3. Also at the first three sampling stations in box 3 (Table 11), the first moment values for tritium are greater than those for naphthalene indicating flow faster than the water. The cause of this behavior is not known at this time.

Column Experiment

Two glass column experiments were conducted, but only the nonreactive bromide tracer, was observed in the first experiment. The lithium was so diluted that it was not detected by the analytical procedure. The breakthrough curves for bromide and lithium from both experiments are given in Figures 5-7.

In both experiments, the bromide breakthrough was well behaved. In experiment 2 (Figure 6) there is an appearance of asymmetry in the bromide breakthrough curve. In experiment 1, the bromide peak was quite rapid due to the dilution (Figure 5). Also, some problems with the specific ion electrode for bromide caused fluctuations in the values. The problem was corrected prior to the second experiment. The lithium pulse in Figure 7 reveals irregular behavior such as multiple peaks over the experimental duration.

Temporal moments were used on the glass columns because data were available only for the input and effluent ends. The algorithm is the same Gauss-Legendre routine used to analyze the centerline data from the box experiments. Temporal moment data from the glass column experiments are given in Table 12. Obvious differences in retardation of lithium versus the naphthalene by the Columbus Air Force Base aquifer material can be seen in Box 3 experiment. For the glass column, the ratio of the first moment for lithium to that for bromide is 3; for either the spatial moments (Table 3) or the centerline temporal moment analysis (Table 11) for box 3, the naphthalene retardation was between 1.0 and 1.2. The differences are obviously due to different retardation mechanisms for the two compounds. Differences in the bromide pulses between for the two column experiments are due to (1) problems in controlling flow rate, (2) correcting the electrode problem in experiment 2, (3) differences in input duration (3 hrs versus 6 hrs), and (4) target concentration (100 mg/L for exp. 1 versus 850 mg/L for exp. 2).

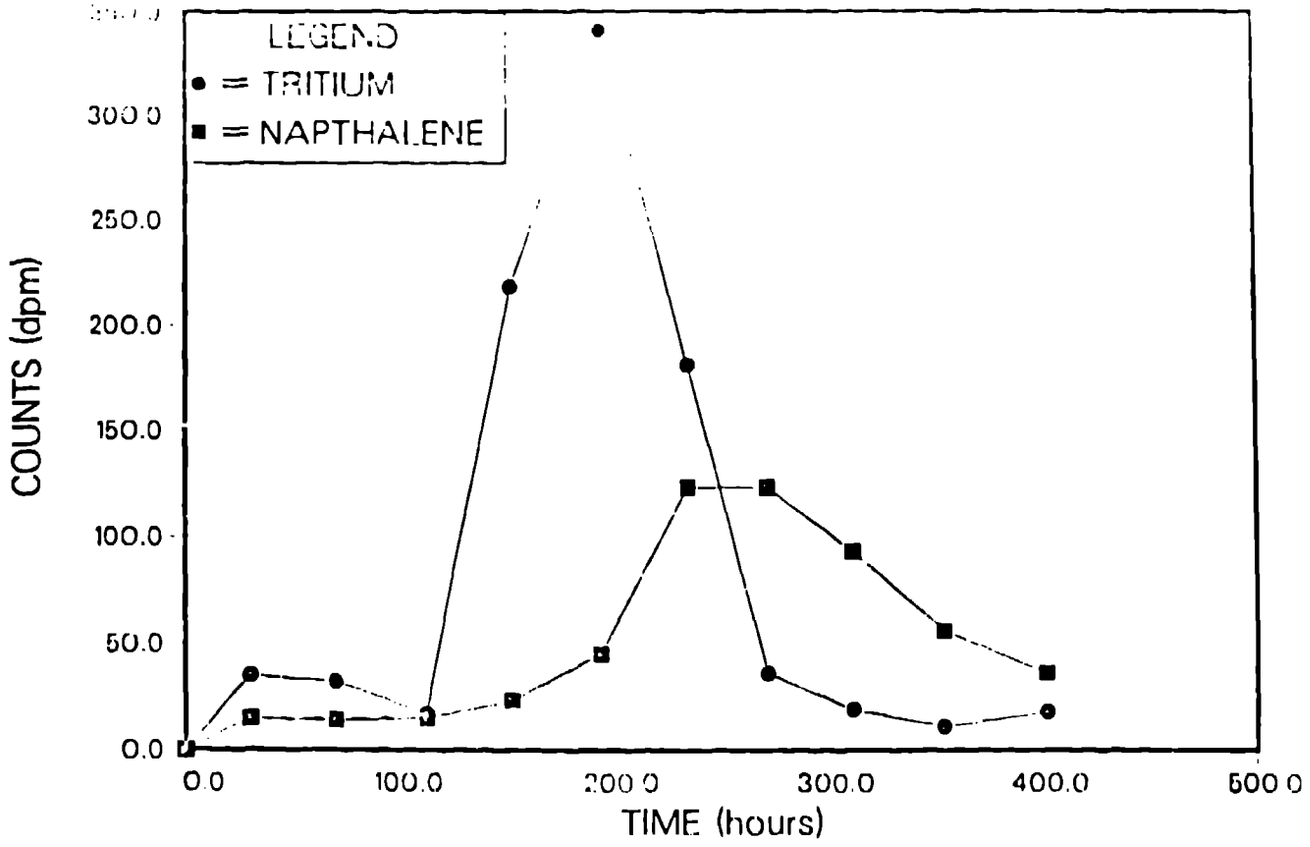

Figure 4. Breakthrough curves for tritium and naphthalene from box 2 sampling well located at x = 60.33 cm and y = 15.24 cm.

Table 9. First and second normalized temporal moments for centerline sampling wells from box 1.

	TRITIUM		NAPHTHALENE	
X (cm)	M1 (hr)	M2 (hr^2)	M1 (hr)	M2 (hr^2)
20.32	7.11	103.15	10.42	276.72
30.16	9.23	105.84	15.60	467.47
40.32	13.08	225.67	17.89	486.31
50.17	25.18	1129.88	28.74	1180.71
60.33	20.20	452.90	26.60	827.52
70.17	23.51	593.32	31.79	1158.76
80.33	31.84	1111.94	40.35	1957.81
90.49	30.79	984.97	39.75	1685.43
100.65	35.29	1276.68	43.82	2005.15
110.81	37.64	1456.51	47.59	2353.49
120.33	41.63	1768.55	50.61	2631.59
130.18	45.52	2097.86	54.07	2972.26

Table 10. First and second normalized temporal moments for centerline sampling wells from box 2.

	TRITIUM		NAPHTHALENE	
X (cm)	M1 (hr)	M2 (hr^2)	M1 (hr)	M2 (hr^2)
20.32	68.09	7855.7	83.91	11455.7
30.16	104.04	14677.2	123.07	19655.6
40.32	131.03	21083.94	162.85	30981.0
50.17	197.51	48454.64	213.41	56904.0
60.33	189.91	40128.86	257.16	72796.0
70.17	226.59	55279.54	273.50	82469.0
80.33	243.20	68796.01	248.55	73433.0
90.49	291.04	89571.84	276.78	88216.0
100.65	310.13	102389.18	259.68	79966.0
110.81	323.33	111824.02	238.37	69800.0
120.33	304.27	104139.40	239.95	70670.0
130.18	272.95	88833.84	235.76	69662.0

Table 11. First and second normalized temporal moments for centerline sampling wells from box 3.

	TRITIUM		NAPHTHALENE	
X (cm)	M1 (hr)	M2 (hr^2)	M1 (hr)	M2 (hr^2)
20.32	105.25	33466.1	84.07	9719.4
30.16	96.26	11535.0	75.60	7606.7
40.32	80.01	8459.6	76.45	7748.4
50.17	97.00	10668.0	100.34	11216.0
60.33	94.56	10825.0	109.95	13766.0
70.17	111.74	14178.0	125.94	17031.0
80.33	117.94	15393.0	129.44	17881.0
90.49	125.43	17084.0	127.17	17439.0
100.65	125.71	17103.0	129.43	18109.0
110.81	129.60	18031.0	134.52	19381.0
120.33	131.17	18422.0	136.42	19936.0
130.18	131.73	18738.0	132.14	1[illegible]240.0

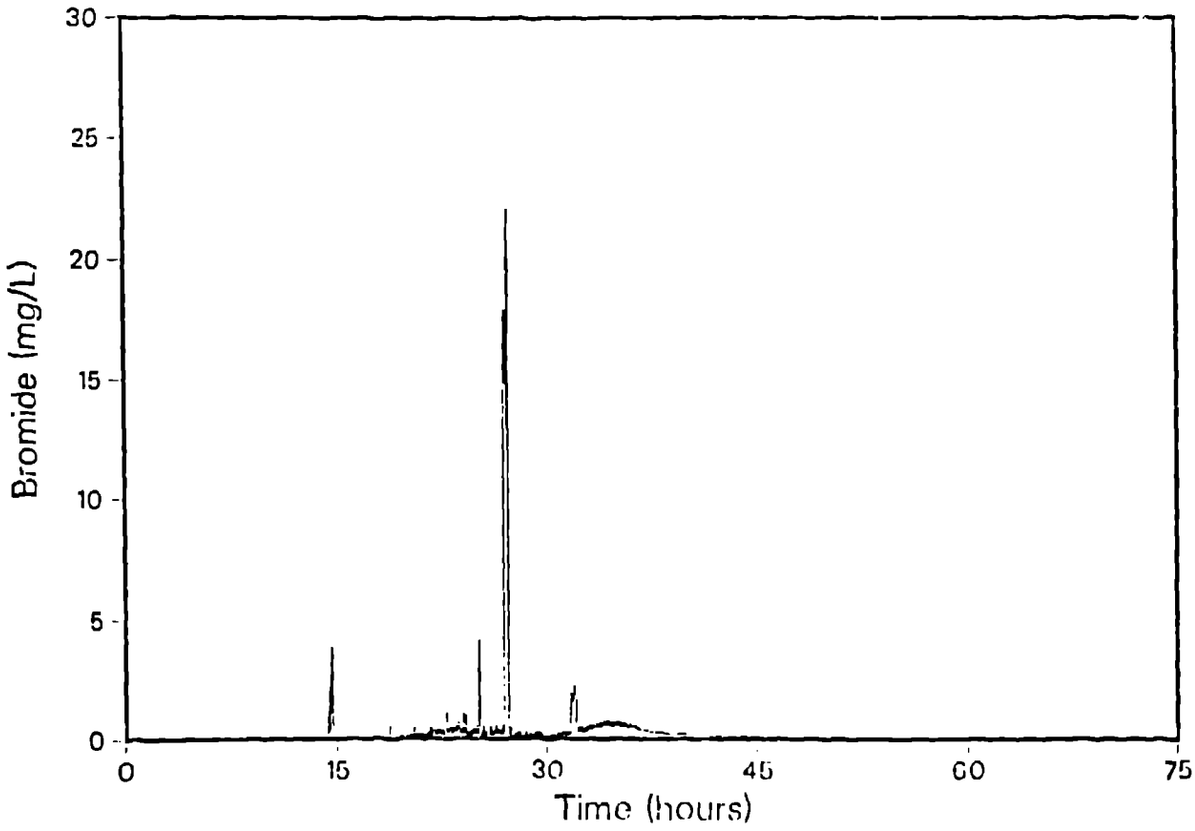

Figure 5. Bromide breakthrough curve for the first glass column experiment.

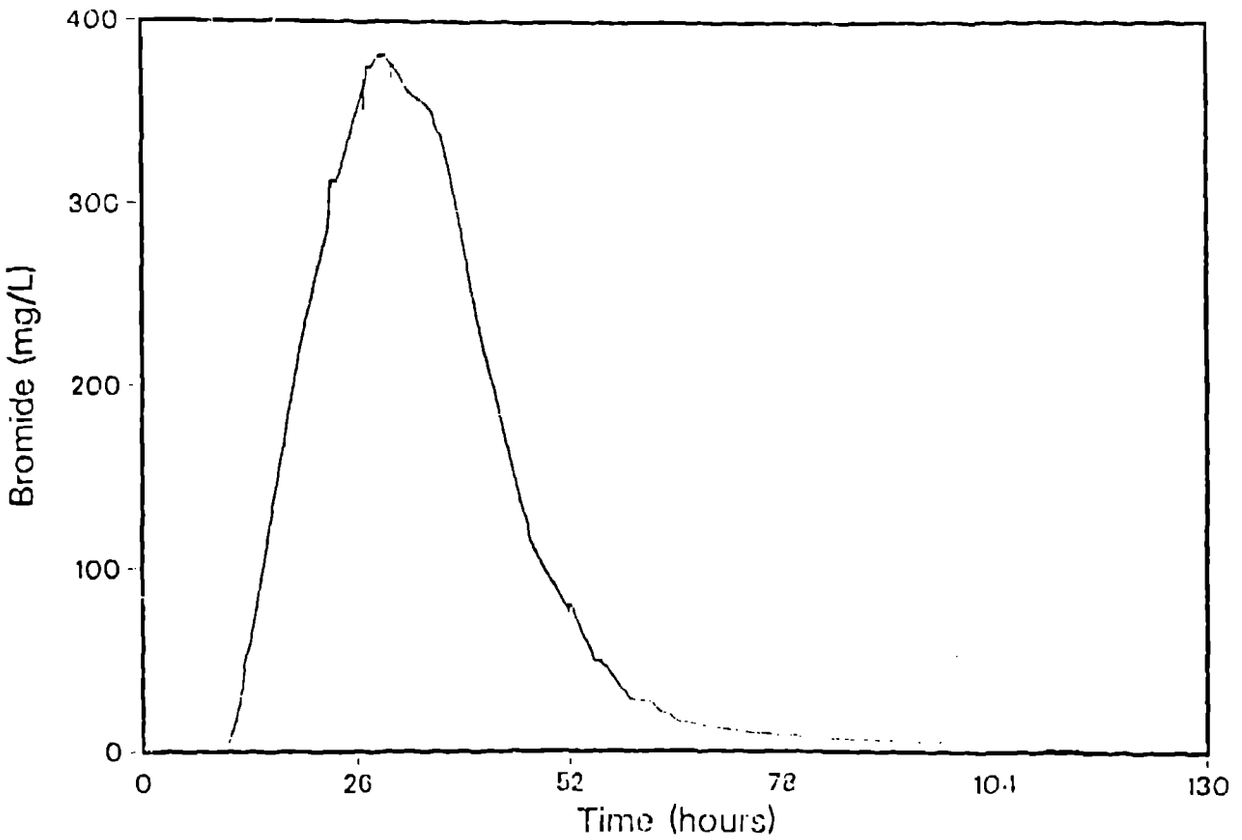

Figure 6. Bromide breakthrough curve for the second glass column experiment.

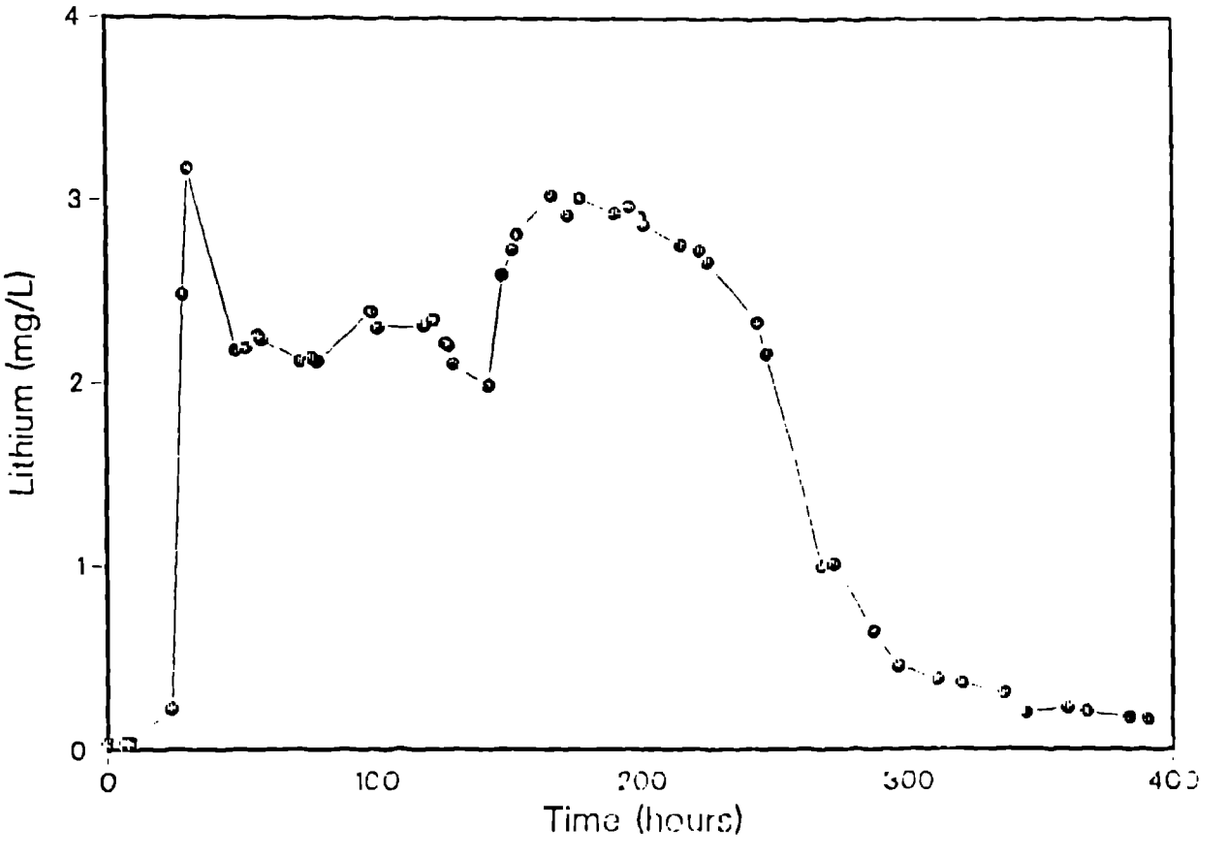

Figure 7. Lithium breakthrough curve for the second glass column experiment.

Table 12. Normalized first and second temporal moments for the 1-meter long glass column experiments.

	BROMIDE		LITHIUM	
Experiment	M1 (hr)	M2 (hr^2)	M1 (hr)	M2 (hr^2)
1	29.2	889.0	[1] --	--
2	34.2	1363.5	117.7	23163.1

[1]No lithium observed experiment 1.

DISCUSSION

When making comparisons between the box and column results one must keep in mind the fundamental differences between the two experimental approaches. The column experiments represent a one-dimensional flow system. The box experiments on the other hand are basically one-dimensional in terms of flow, but the solute has the potential for three-dimensional spreading. The column approach represents the more traditional method for determining transport parameters for field efforts, but field conditions are more multidimensional. Information from the spatial moments indicated very little lateral spread in the box experiments. The vertical movement was unknown.

The differences in velocities for the three box experiments were given in Table 4. To recap these results, the differences in velocity between box 1 and box 2 did not affect the retardation of the naphthalene. The change from sand to the Columbus AFB aquifer material in box 3 resulted in a lower retardation.

The box and column experiments cannot be compared in terms of the retardation because naphthalene or lithium were not used in both experiments, but the transport parameters can be compared. Using the column length of 85 cm the first and second moments given in Table 12 for the column are consistent with the centerline temporal moments for tritium for the 80.33-100.65 cm sampling distances from box 1 (Table 9). A test of the applicability of the data from the column to the box would be to predict the behavior at a lower velocity such as box 3. In this case, the lower velocity is expected to lead to more spreading of the plume.

Up to this point, no model has been assumed for governing the transport in either of these two systems. In application, the advection-dispersion equation would normally be assumed to describe the migration of a contaminant. The advection-dispersion equation is written as:

$$\frac{\partial c}{\partial t} = \frac{\partial}{\partial x}\left[D \frac{\partial c}{\partial x}\right] - \frac{\partial Vc}{\partial x}$$

where c is the solute concentration (m/L**3); D is the dispersion tensor (L**2/T); V is the pore water velocity (L/T); t is time (T); and X is the spatial coordinates (up to 3) (L). If Equation 5 is assumed, Freyberg (1986) and Turner (1972) have shown how the spatial and temporal moments can be used to estimate the parameters V and D. Bear (1979) provides a general relationship for the components of the dispersion tensor and velocity in three-dimensions. These relationships reduce to the following for flow parallel to the X-coordinate direction and when diffusionis ignored:

$$D_x = dl * V$$

$$D_z,\ D_y = dt * V$$

where D_x, D_y and D_z are the dispersion coefficients (L^2/T), dl is the longitudinal dispersivity (l); dt is the transverse dispersivity (l); and V is

the velocity in this case parallel to the X-coordinate direction (L/T). The dispersity is a length scale of the porous medium that describes the spreading of a plume in relation to the velocity. By deriving the dispersivity for bromide from the column experiments and attempting to predict the tritium response in box 3 using athe column based value, a comparison of the column results with the box results can be conducted. The comparison of velocity is not assumed important because velocities will change depending on the field conditions. If the relationships in Equation 6 hold, then a reasonable estimate of behavior in the box experiment using values from the column experiment should be possible.

The solution to equation 5 for this test was taken from Hunt (1978) for an instantaneous point injection (Hunts equation 10). This solution is :

$$C(x,y,z,t) = M_3 \exp \frac{\left[\frac{(x - Vt)^2}{4Dxt} - \frac{y^2}{4Dyt} - \frac{z^2}{4Dzt}\right]}{8\phi\sqrt{\pi^3 t^3 D_x D_y D_z}}$$

where M_3 is the injected mass(M**3); ϕ is the porosity; x, y, and z are the coordinates (L); and all other variables and parameters are as defined. The estimate for velocity in equation 7 is the average velocity for box 3 from Table 4.

To estimate dl in equation 6a, the relationship for temporal moments from Turner (1972) will be used:

$$V = (Z/(M_1 - T_0/2)$$

where V is the velocity (L/T); Z is the sampling distance 'L); M_1 is the first normalized temporal moment (t); and $T_0/2$ is the correction for the square wave input pulse. T_0 is the input pulse duration. D_x is estimated using the following equation from Turner (1972):

$$D_x = \frac{\left[\frac{M_0 M_2}{M_0} - (M_1)^2\right] - \frac{T_0^2}{12} * V^3}{2Z}$$

Where M_0 is the zero moment; M_2 is the second moment; M_1 is the first moment; T_0 is the input pulse duration; V is from Equation 8; and Z is the sampling length. Note that the raw moments are used in Equations 8 and 9.

The values for dl from column 1 was 2.2 cm, and for column 2 dl was 8.3 cm. Differences between these values can be due to differences in injection

time, flow rate fluctuations, and instrument stability. Values for dt were not obtained from the column experiments so the assumption that dt=0.1*dl was used.

To match the results from the column, the 100.65-cm sampling distance in box 3 was used because after correcting for the 15.2 cm distance for the injection well, this value best represents the 85-cm sampling distance of the column. The comparison of the observed data with the predictions from the column can be seen in Figure 8. The prediction with the column 1 dl shows a delayed response and a higher peak than was observed. The column 2 dl causes greater dispersion with a highly damped breakthrough curve. The delayed response in the curve from column 1 in Figure 8 may have been due to using the average velocity rather than the velocity calculated using the first moment data from Table 12 and Equation 8. Figure 9 results when this revised velocity value is used and the column 1 data provides a better fit to the observed data.

There are difficulties as shown by this small scale demonstration in transferring information on transport between systems of different dimensions. Domenico and Robbins (1984) noted this in their model study and they found that scale dependency in the dispersion coefficient is induced by using lower dimensional models to describe a higher dimensional system. In field situations the effects of heterogeneities in the flow field can cause further dispersion that is included in the dispersion coefficient but not in the velocity term.

Application of models to remedial actions such as pump and treat must be able to deal with uncertainties such as that shown here in order to be effective. The range in dl between the two column experiments is not large but the effects of a given location can be substantial as shown in Figure 8. Also, the importance of accurate estimates of key parameters is demonstrated in Figure 9.

SUMMARY AND CONCLUSIONS

Two experimental approaches were used to examine transport in porous media. The box design allowed two-dimensional sampling of the plume. The more traditional column design was one-dimensional with measurements only of the effluent. The method of moments was applied to describe tracer response using spatial and temporal moments for the box results, and temporal moments for the column results.

An attempt was made to predict nonreactive tracer behavior for a box experiment containing Columbus AFB aquifer material using parameters from the column experiments. There was little correspondence between observed and predicted responses. Further investigations are underway at both laboratories to investigate further the behavior of contaminants at various scales. At AFESC, the sampling design of the box experiments was altered to provide a three-dimensional network by installing multiple samples at a given x y location with different depths. At Los Alamos, a larger column that is 1 m in diameter and 3 m long will be used in addition to an improved version of the 1-m long column used in this experiment. By conducting studies on similar porous materials at different scales, a more unified approach of moving from laboratory to the field can be developed. This will provide more confidence in using models to assess field conditions.

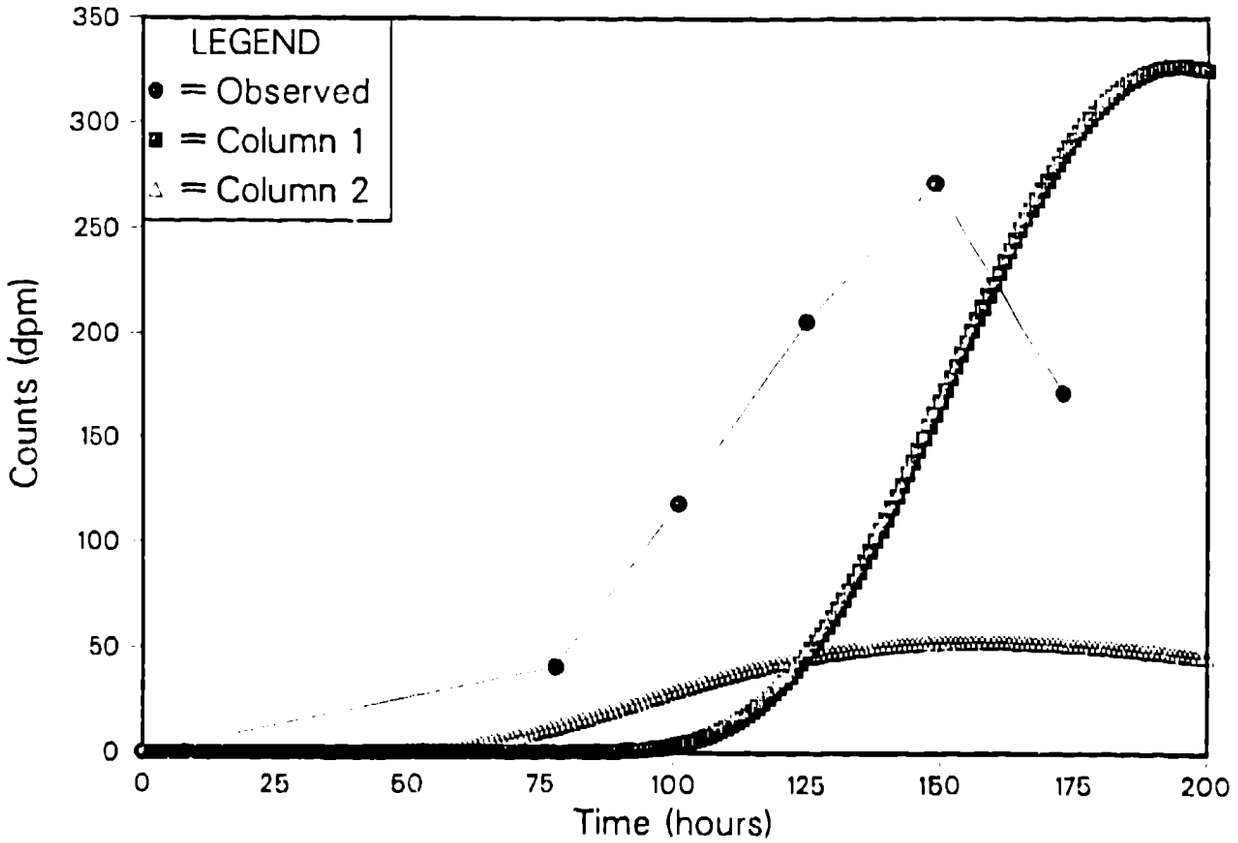

Figure 8. Comparison of observed tritium breakthrough in box 3 at x = 100.65 cm and y = 15.24 cm with curves predicted using parameters from glass columns 1 and 2.

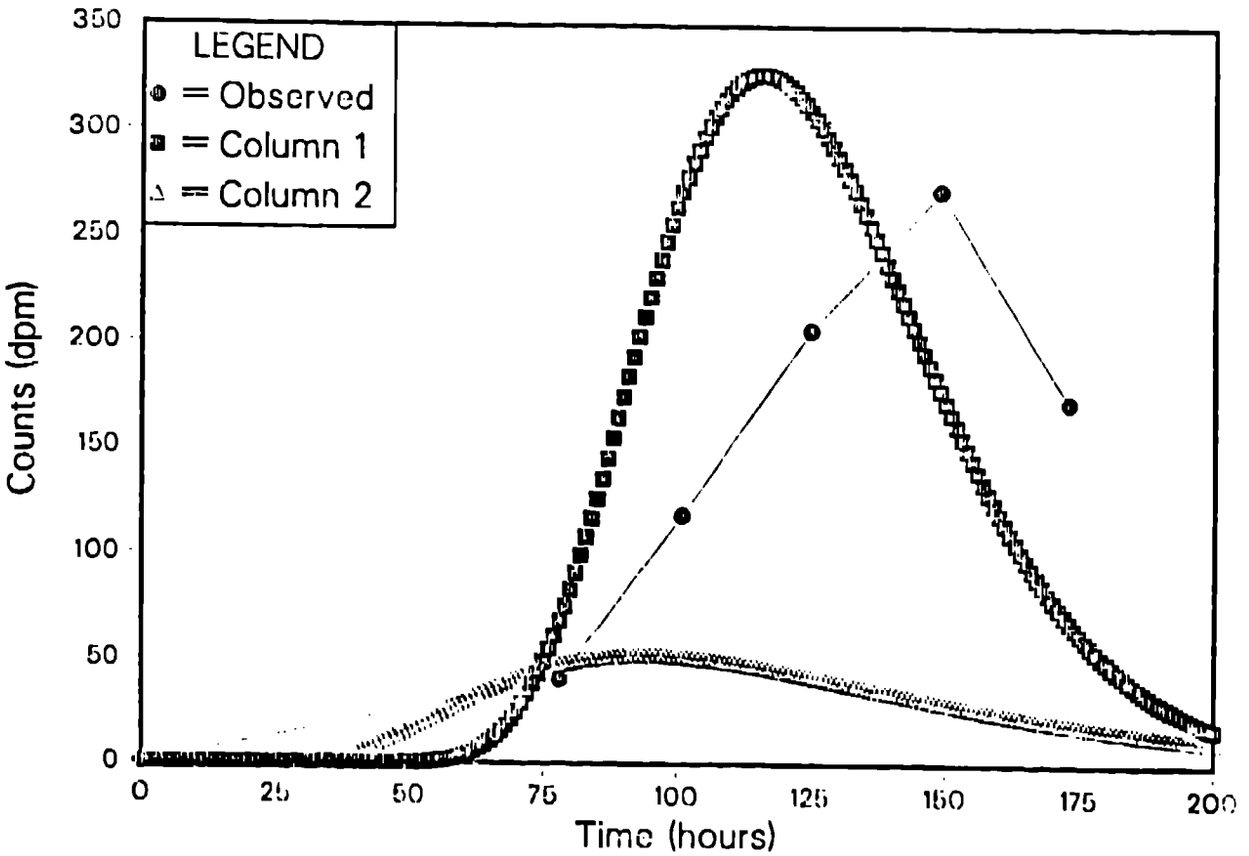

Figure 9. Comparison of observed tritium breakthrough in box 3 at x 100.65 cm and y 15.24 cm with curves predicted using parameters from glass columns 1 and 2 and the observed velocity from temporal moments of box 3.

ACKNOWLEDGEMENTS

Funding to Los Alamos for this study was provided by the Air Force Engineering Services Laboratory. Special thanks to G. Langhorst, C. Pruvost, and S. gonzales for help in preparing this manuscript. Los Alamos National Laboratory is operated by the University of California for the U. S. Department of Energy under contract W-7405-ENG-36.

LITERATURE CITED

Abramowitz, M., and I.A. Stegun, eds. 1972. Handbook of mathematical functions. Dover Pub., New York, NY, 1046 pp.

Bear, J. 1979. Hydraulics of groundwater. McGraw-Hill, NY, 569pp.

Carnahan, B., H.A. Luther, and J.O. Wilkes. 1969. Applied numerical methods. John wiley and Sons, New York, NY, 604pp.

Domenico, P.A., and G.A. Robbins. 1984. A dispersion scale effect in model calibrations and field tracer experiments. J. Hydrol., 70:123-132.

Freyberg, D.L. 1986. A natural gradient experiment on solute transport in a sand aquifer 2. Spatial moments and the advection and dispersion of nonreactive tracers. Water Resour. Res., 22(13):2031-2046.

Hunt, B. 1978. Dispersive sources in uniform ground-water flow. J. Hydraul. Div., Am. Soc. Civil Eng., 104:75-85.

Mackay, D.M., D.L. Freyberg, P.V. Roberts, and J.A. Cherry. 1986. A natural gradient experiment on solute transport in a sand aquifer 1. Approach and overview of plume movement. Water Resour. Res., 22:2017-2029.

Turner, G.A. 1972. Heat and concentration waves. Academic Press, NY, 233p.